

Distance to the Messier 52 Cluster

Jonathan Pal, Josiah Castillo, and Dillon Peng

December 7, 2021

Abstract

Messier 52, is an open galactic cluster. The author measured the distance to the M52 cluster using Hertzsprung–Russell (HR) diagram analysis, and a known measurement of the distance to the Messier 11 (“Wild Duck”) cluster. The author determined that the distance to the Messier 52 is approximately 1100 ± 151 parsecs, under the assumption that the Wild Duck cluster is 1814 ± 63 parsecs away. The uncertainties quoted here are 1σ . Literature suggests that the actual distance to Messier 52 is about 1350 parsecs. Various sources of uncertainty are discussed.

1 Introduction

The following table summarizes some key information which the reader may want to know about the M52 cluster [Str]:

Property	Value
Name 1	M52
Name 2	NGC 7654
Class	Open Galactic Cluster
Right Ascension	23 24 46.8
Declination	+61 35 24
Angular Size	16 arcminutes

Figure 1: Properties of the Messier 52 cluster.

A similar table for the Wild Duck cluster is below [Strb]:

Property	Value
Name 1	M11
Name 2	NGC6705
Nickname	Wild Duck cluster
Class	Open Galactic Cluster
Right Ascension	18 51 03.8
Declination	-06 16 19
Angular Size	8.9 arcminutes
Distance 1	1750 parsecs
Distance 2	1877 parsecs

Figure 2: Properties of the Wild Duck cluster.

Since it is of particular importance to this project, note that the distance measurements cited by [Strb] originate from [DSP17] and [Kha+05], respectively. No indication of the uncertainty in either distance measurement is provided. For purposes of this project, it will be assumed that the distance to the Wild Duck cluster is 1814 ± 63 parsecs.

1.1 Equations Utilized

In the paper, a two basic mathematical relations from astronomy will be utilized. For convenience of both the author and reader, they are numbered here for reference:

$$F \propto r^{-2}, \quad (1)$$

where F is flux, and r is radial distance from a celestial object.

$$r_{0\lambda} \approx 0.2 \frac{\lambda}{\theta}, \quad (2)$$

where $r_{0\lambda}$ is the Fried parameter, λ is the central wavelength of the filter used in microns, and θ is the Full Width at Half Max in arcseconds.

2 Experimental Procedure

The author's group's measurements utilized the CCD camera at the 0.8m Krizmanich Telescope at the Jordan Observatory at Notre Dame. The author's group had already obtained 20 flat frames and 70 bias frames in a previous project. When these flats were taken, the author's group's intention was to take the flat frames at twilight, but ultimately most flat frames were taken when the sky was darker than they would have preferred, making them suboptimal. Since the exposure length used for this project was different than their previous project, the author's group took new dark images which had the same length as their science images. Specifically, for each of the two exposure lengths used for the science images, 10 dark images were taken. More specific information about the observations can be found in the observing log in Appendix A.

For both clusters, the author's group utilized three filters: Red (R), Blue (B), and Visual (V). This was intended so that the authors would be able to obtain a basic indication of the spectrum of the stars in the cluster, which was vital for the analysis in Section 4.1.2.

2.1 Calibration

The following table gives the exposure length and number of frames for the various types of science frames taken:

Cluster	Filter	Exposure Length	# of Frames
Wild Duck	B	5 sec	20
Wild Duck	V	5 sec	20
Wild Duck	R	5 sec	20
M52	B	30 sec	10
M52	V	30 sec	10
M52	R	30 sec	10

Figure 3: Information about science frames.

These exposure lengths were optimized to obtain a strong signal to noise ratio without reaching a nonlinear part of the CCD. This optimization was performed by trial and error, with different exposure times tested, and then the maximum pixel values compared against known measurements for where the Krizmanich's CCD becomes nonlinear. The author's group also made qualitative measurements of the level of saturation by observing the images at different exposure times and looking for signs of saturation in bright stars. The author's group noted on the night of their observation that the quantitative and qualitative measurements were in reasonable agreement with one another, and thus are reasonably confident that the images have a sufficiently large exposure time to obtain a strong signal to noise ratio while not introducing nonlinearity in measurements.

Following the conclusion of their observations, the science images that the author's group obtained were calibrated using MaximDL. In particular, the additive effects were removed by subtracting the mean of the dark images. The dark images did not appear to have significant outliers, so the mean seemed to be an accurate representation of the dark current. Since the dark images had the same exposure time as the science images (multiple exposure lengths were taken for darks), it was not necessary to use the bias images during the removal of additive effects from

3 Results

The following graph is a B-V HR diagram for M52:

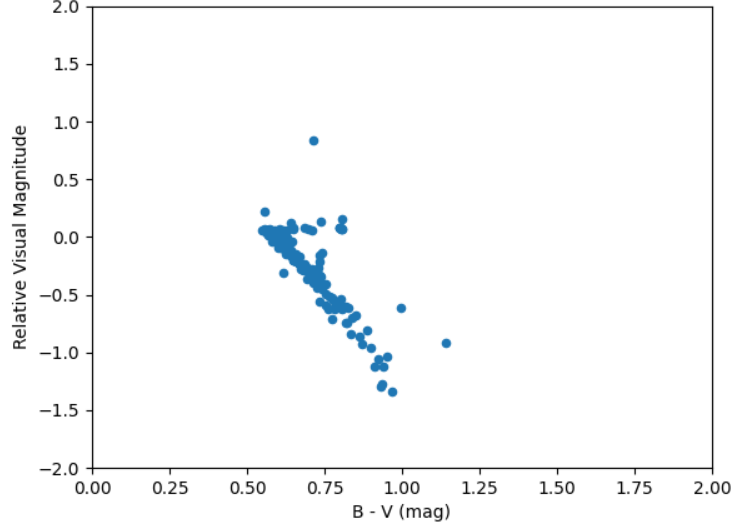


Figure 6: Visual magnitude vs. Color for stars in the M52. This is a subset of a larger graph; points outside of the ranges seen on the x and y axes were deemed outliers. The zero on the y-axis is defined as the median of all of the magnitudes (including the outliers discarded).

A similar diagram is below for the Wild Duck Cluster:

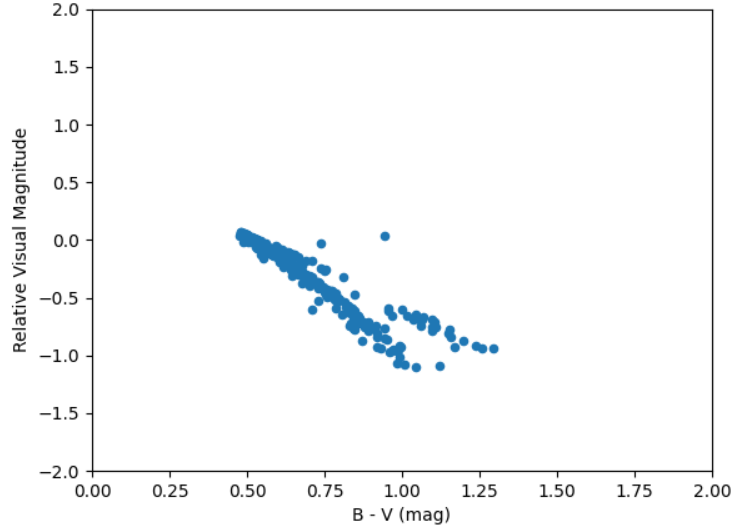


Figure 7: Visual magnitude vs. Color for stars in the Wild Duck cluster. This is a subset of a larger graph; points outside of the ranges seen on the x and y axes were deemed outliers. The zero on the y-axis is defined as the median of all of the magnitudes (including the outliers discarded).

Additional HR diagrams were created using B-R and V-R on the x-axis. While the above diagrams are illustrative for understanding the general shape of the HR diagrams and the analysis process, the interested reader may find the additional HR diagrams in Appendix D.

4 Analysis & Discussion

4.1 Calculation of Distance

The goal of analysis was to solve for the ratio c as defined by the following equation:

$$\text{Distance to M52} = C \cdot \text{Distance to the Wild Duck Cluster.} \quad (3)$$

Since the distance to the Wild Duck cluster is taken to be a known value, if C is calculated, then the distance to M52 can be calculated. To calculate C , the author computed visual magnitude as a function of color.

4.1.1 Calculation of Flux

The first step for each master image was to estimate the FWHM of the image. This was done by identifying a large number of unsaturated stars with [BCS20], and then approximately identifying their peak flux, and then identifying the radial distance from the center of the PSF at which the values are most nearly half of the peak [Pald]. The estimated FWHM and $r_{0\lambda}$ for each master science image is presented below:

Cluster	Filter	FWHM (pix)	FWHM (arcsec)	$r_{0\lambda}$ (centimeters)
Wild Duck	B	10.6 ± 3.6	8.28	1.00
Wild Duck	V	8.01 ± 3.4	6.25	1.66
Wild Duck	R	7.96 ± 3.5	6.21	1.93
M52	B	16.3 ± 4.6	12.7	0.65
M52	V	14.2 ± 3.4	11.1	0.94
M52	R	12.7 ± 2.4	9.91	1.21

Figure 8: FWHM and Fried parameter, measured for both clusters in all filters. The uncertainty given for FWHM is 1σ . The FWHM in arcseconds was calculated using a pixel scale of 0.78 arcsec/pixel. The Fried parameter was calculated using Equation (2).

Obviously, the Fried parameter much smaller than the aperture of the Krizmanich Telescope in all cases, so the observations are seeing limited rather than diffraction limited. As is perhaps well known, the seeing in South Bend is rather poor; these measurements corroborate that. The differences in the Fried parameter for different images are both a result of differences between the seeing conditions throughout the night and

After an estimate of the FWHM, flux measurements were made for a large number of stars using circular apertures¹ whose radius was half of the FWHM [Pald]. First, the stars' locations were identified, then their PSFs were deblended [BCS20]. During this process, a Gaussian kernel was applied [Ast+18]. After their PSFs were deblended, the circular apertures were applied to measure the flux. The flux was normalized by the area of the aperture. After the fluxes were found in each master image, the correspondence between flux measurements in different images was calculated [BCS20], and a singular table was produced containing the flux in B, flux in V, and flux in R for each star [Palc]. The reader may find the flux measurements in Appendix B and Appendix C if they are interested.

4.1.2 Calculation of Distance Ratio

The paragraph after the following paragraph will describe the analysis process using the difference in B magnitude and V magnitude as the value for color (x-axis in HR diagram). The process was also conducted using the difference in B magnitude and R magnitude and the difference in V magnitude and R magnitude, and the distance ratios calculated from each of these was averaged to yield the value of C (as defined in Equation (3)) to be 0.6065 ± 0.02 [Pala]. The uncertainty given is 1σ . Using this value for C , and 1814 ± 63 parsecs as the distance to the Wild Duck cluster, Equation 3 indicates that the distance to the M52 cluster is approximately **1100 \pm 151 parsecs**.

Once all of the flux measurements were made, outliers were discarded. "Outlier" was defined as being more than 2 magnitudes away from the median visual magnitude (y-axis in HR diagram), or having a difference in B magnitude and V magnitude less than 0 or greater than 2. The points

¹The author utilized [Bra+20] for aperture photometry.

which were not considered to be outliers are exactly the points which are portrayed in Figures 7 and 6. These points appeared to the author to loosely constitute the shape of a parabola, so the author fit a second degree polynomial to the data points in each image. The author then took 50000 points off of this curve and used these points to calculate the flux of best fit for a star with some particular color in each cluster. Then, the corresponding points from each cluster were divided, and the square root of this ratio was taken. Using the assumption that luminosity is a function of color and in accordance with Equation (1), this gives an indication of the ratio between the distances between the two clusters. The average of each of these calculated ratios was taken to give an estimate on the value of C . The interested reader can find details in [Pala].

4.2 Sources of Uncertainty

1. The Poisson uncertainty (\sqrt{N}) is unavoidable independent of experimental procedure. However, this does not appear to be a major source of error in the photometry measurements.
2. Return to the remark in Section 2 regarding the quality of the flat frames. It was remarked earlier that the flat frames had a considerable amount of variation, and it was suggested that this was due to the flat frames being taken too late after dusk such that the sky was no longer uniform in the region in which the telescope was pointed. That there is a considerable amount of variation is confirmed by a statistical analysis on the flat images taken. In particular, for each pixel, the ratio of the median absolute deviation of the values of that particular pixel across the flat images to the median of the values of that particular pixel was calculated [Palb]. Written mathematically, for some pixel (i, j) , say $m = \text{median}\{\text{image}[i, j] : \text{image} \in \text{flat images}\}$. Then the calculated value for that pixel is

$$\frac{\text{median}\{|\text{image}[i, j] - m| : \text{image} \in \text{flat images}\}}{m}$$

It was measured that the mean of this calculated value across all 1048576 pixels was **35.9%**. This indicates a very significant variation in the flat images taken. Since the flat images were taken in close proximity to one another (both temporally and spatially), this indicates that the region of sky which the flats were taken over was likely not a very uniform region, making the flats fairly unreliable. Hence the calibration described in Section 2.1 is unreliable with respect to multiplicative effects.

3. Since the reliability of the flats has been discussed, it is fitting to discuss the reliability of the darks and biases as well. For these, since a mean was used rather than a median, the ratio calculated for each pixel was the ratio of the standard deviation (rather than median absolute deviation) to the mean. In the case of the darks, the mean of this calculated value across all pixels was 0.630%, and in the case of the biases, the mean of this calculated value across all pixels was 0.603%. This indicates that the darks and biases are very consistent, as would be expected given that they were taken back to back and the dark current and bias in a CCD device does not change very quickly over time. Thus the calibration described in Section 2.1 is reliable with respect to additive effects.
4. Return now to the assumption that the distance to the Wild Duck cluster is 1814 parsecs. The two sources are in reasonable agreement, but no indication of the uncertainty in either measurement is given. Based on the two measurements, the distance to the Wild Duck cluster has at minimum an uncertainty of 64 parsecs (3.53%), although an understanding of the uncertainties in each of these measurements would yield a more concrete understanding of the uncertainty in the calculation which their mean was used for.
5. Return to Figure 5. The reader can easily see that the stars are very crowded. Consider this in conjunction with the Fried parameter calculations in Figure 8. These measurements indicate very poor seeing on the night that the observations were made. As such it is the case that close objects cannot be well-resolved. As such, there is potentially considerable error in the flux measurements. With that said, a couple elements of the process probably mitigated the error produced by the seeing limitation. First, when the distance measurements were made, outliers were discarded. Second, when flux measurements were made, the aperture radius was small ($\frac{\text{FWHM}}{2}$). Should the author have had more time, this radius could have been better optimized, but it is probably a reasonable radius for the apertures.

4.3 Literature

Simbad [Stra] indicates that the distance to the M52 cluster is approximately 1350 parsecs. This value is taken from [DSP17]. No estimate on the uncertainty in this measurement is provided. There is an 18% difference between the measurement described in Section 4.1.2 and this literature value. This seems like a reasonable discrepancy given the multitude of potential sources of error described in Section 4.2 and the likely uncertainty in the literature value cited by Simbad.

The reader should notice, however, that the amount of uncertainty indicated by the standard deviation in measurements of C does not account wholly for this discrepancy. If the literature value is taken to be reliable, this indicates a systematic error in the author’s process. One conspicuous possibility for this is the assumption that the distance to the Wild Duck cluster is 1814 parsecs. The distance measurements cited by Simbad for the Wild Duck cluster do not indicate sufficient uncertainty for this to be a sufficient explanation (they were included in the calculation made in Section 4.1.2), but Simbad only quotes two sources, hence the introduction of more literature values may demonstrate sufficient uncertainty in the literature as to the distance to the Wild Duck cluster to account for this discrepancy. It is also possible that the second degree polynomial fit described in Section 4.1.2 causes a systematic underestimate of C . It is also worth noting that the quoted value for uncertainty is 1σ , and the use of 2 or more σ as the uncertainty would account for the discrepancy.

5 Conclusion

The author measured the distance to the M52 cluster using Hertzsprung–Russell (HR) diagram analysis, and a known measurement of the distance to the Messier 11 (“Wild Duck”) cluster. The author determined that the distance to the Messier 52 is approximately 1100 ± 151 parsecs, under the assumption that the Wild Duck cluster is 1814 ± 63 parsecs away. It was noted that the author’s calculations indicate a lesser degree of uncertainty in the measurement than the literature would suggest. It has been argued that systematic error is present in the data. It is suggested that a more thorough survey of the literature on the distance to the Wild Duck cluster be conducted such that the uncertainty in the current literature is better known. It is also suggested that the data be analyzed again using a couple other justifiable analysis pathways, such that it may become clear whether there is a systematic error generated by the author’s process.

References

- [Kha+05] Kharchenko, N. V. et al. “Astrophysical parameters of Galactic open clusters”. In: *A&A* 438.3 (2005), pp. 1163–1173. DOI: [10.1051/0004-6361:20042523](https://doi.org/10.1051/0004-6361:20042523). URL: <https://doi.org/10.1051/0004-6361:20042523>.
- [DSP17] Sami Dib, Stefan Schmeja, and Richard J. Parker. “Structure and mass segregation in Galactic stellar clusters”. In: *Monthly Notices of the Royal Astronomical Society* 473.1 (Sept. 2017), pp. 849–859. ISSN: 0035-8711. DOI: [10.1093/mnras/stx2413](https://academic.oup.com/mnras/article-pdf/473/1/849/21370814/stx2413.pdf). eprint: <https://academic.oup.com/mnras/article-pdf/473/1/849/21370814/stx2413.pdf>. URL: <https://doi.org/10.1093/mnras/stx2413>.
- [Ast+18] Astropy Collaboration et al. “The Astropy Project: Building an Open-science Project and Status of the v2.0 Core Package”. In: 156.3, 123 (Sept. 2018), p. 123. DOI: [10.3847/1538-3881/aabc4f](https://doi.org/10.3847/1538-3881/aabc4f). arXiv: [1801.02634](https://arxiv.org/abs/1801.02634) [astro-ph.IM].
- [BCS20] M. Beroiz, J.B. Cabral, and B. Sanchez. “Astroalign: A Python module for astronomical image registration”. In: *Astronomy and Computing* 32 (2020), p. 100384. ISSN: 2213-1337. DOI: <https://doi.org/10.1016/j.ascom.2020.100384>. URL: <http://www.sciencedirect.com/science/article/pii/S221313372030038X>.
- [Bra+20] Larry Bradley et al. *astropy/photutils: 1.0.0*. Version 1.0.0. Sept. 2020. DOI: [10.5281/zenodo.4044744](https://doi.org/10.5281/zenodo.4044744). URL: <https://doi.org/10.5281/zenodo.4044744>.
- [Pala] Jonathan Pal. *distance_measurement.py*. URL: https://github.com/JonathanDPal/wildduck/blob/main/distance_measurement.py. (accessed: 12.06.2021).
- [Palb] Jonathan Pal. *error.py*. URL: <https://github.com/JonathanDPal/wildduck/blob/main/error.py>. (accessed: 12.01.2021).
- [Palc] Jonathan Pal. *flux_matching.py*. URL: https://github.com/JonathanDPal/wildduck/blob/main/flux_matching.py. (accessed: 12.06.2021).
- [Pald] Jonathan Pal. *flux_measurement.py*. URL: https://github.com/JonathanDPal/wildduck/blob/main/flux_measurement.py. (accessed: 12.06.2021).
- [Stra] Centre De Données Astronomiques De Strasbourg. *M52*. URL: <http://simbad.u-strasbg.fr/simbad/sim-basic?Ident=M52>.
- [Strb] Centre De Données Astronomiques De Strasbourg. *NGC 6705*. URL: <http://simbad.u-strasbg.fr/simbad/sim-id?Ident=NGC%5C%206705>.

Appendix A: Observation Log

Date	Filenames	Time (UT)	Type	Exp. Time	Filter	Notes
10/6/2021	bias-0001 - bias-0070	00:21 - 00:28	Bias	0	None	
10/26/2021	flats_B_5s-0001 to flats_B_5s-0020	23:13 - 23:16	Flats	5	B	Too dark
10/26/2021	flats_V_20s-0001 to flats_V_20s-0020	23:18 - 23:26	Flats	20	V	Too dark
10/26/2021	flats_R_60s-0001 to flats_R_60s-0015	23:31 - 23:47	Flats	60	R	Too dark
10/27/2021	M52-0001B to M52-0010B	00:27 - 00:35	Science	45	B	Unused
10/27/2021	M52-0001V to M52-0010V	00:36 - 00:43	Science	45	V	Unused
10/27/2021	M52-0001R to M52-0010R	20:44 - 20:52	Science	45	R	Unused
10/27/2021	M52_pt2-0001B to M52_pt2-0005B	00:53 - 00:56	Science	30	B	
10/27/2021	M52_pt2-0001V to M52_pt2-0005V	00:56 - 00:59	Science	30	V	
10/27/2021	M52_pt2-0001R to M52_pt2-0005R	01:00 - 01:02	Science	30	R	
10/27/2021	WildDuck-0001B to WildDuck-0020B	01:15 - 01:19	Science	5	B	
10/27/2021	WildDuck-0001V to WildDuck-0020V	01:19 - 01:22	Science	5	V	
10/27/2021	WildDuck-0001R to WildDuck-0020R	01:23 - 01:26	Science	5	R	
11/17/2021	11-18-dark-0001 to 11-18-dark-0010	00:19 - 00:24	Dark	30	None	
11/17/2021	11-18-dark5-0001 to 11-18-dark5-0010	00:27 - 00:28	Dark	5	None	

Appendix B: Measured Fluxes of M52

X (pix)	Y (pix)	R Flux	B Flux	V Flux
701.7	979.97	20.77	432.26	4.86
77.53	458.96	900.11	4.33	10.85
138.43	34.42	881.41	5.05	11.51
698.2	24.16	879.95	3.77	12.46
67.57	854.57	884.09	3.35	13.03
296.97	59.89	874.49	4.16	13.35
931.13	331.42	858.05	3.75	15.0
1020.53	791.0	488.18	196.84	379.97
187.95	967.54	891.46	400.04	668.91
298.96	182.05	888.46	3.81	699.19
557.04	566.96	894.46	3.92	700.99
394.0	356.99	901.0	2.97	701.56
535.0	316.0	900.53	3.95	701.95
4.95	407.22	920.74	337.84	710.52
436.45	312.96	898.46	3.64	719.91
618.58	678.0	892.62	3.75	719.94
887.92	247.62	916.53	4.37	724.68
5.21	790.96	948.98	368.05	724.88
1017.99	410.26	961.85	404.04	728.24
90.51	234.42	901.09	4.44	738.67
213.54	362.47	895.12	4.3	739.85
977.5	516.57	894.77	4.07	739.99
44.49	500.43	905.11	4.89	740.15
729.53	314.46	892.56	3.34	740.32
33.5	52.0	891.2	6.28	740.37
488.5	382.57	907.38	4.16	740.79
798.54	600.54	890.39	4.32	740.86
304.47	335.47	892.26	5.27	741.88
103.51	993.57	899.46	3.65	742.3
1015.49	747.0	885.08	4.29	743.06
448.0	396.43	901.49	5.86	744.62
889.03	713.91	894.26	3.59	745.84
369.04	226.96	912.49	4.09	746.17
408.44	129.44	926.71	3.82	746.18
992.48	219.53	899.54	4.58	746.27
437.37	220.93	910.57	5.13	746.39
162.95	680.0	905.21	4.94	746.79
604.61	139.13	927.1	12.9	747.15
511.5	440.49	904.17	4.81	747.23
289.44	196.57	914.23	4.63	748.09
446.59	128.46	924.92	3.85	748.28
451.54	300.53	895.37	6.5	748.43
920.97	81.97	908.64	5.26	748.93
827.56	439.56	900.33	5.54	749.04
850.35	441.52	906.76	5.56	749.11
641.0	670.0	914.79	4.59	749.64
876.49	340.44	921.08	3.62	749.84
990.6	542.47	918.14	4.98	749.96
123.47	1005.04	904.49	5.55	750.13
538.65	482.98	918.59	3.29	750.21
201.53	451.04	924.68	4.23	750.23
916.03	479.46	896.13	7.37	750.38
668.85	329.98	910.37	4.09	750.5
581.56	824.55	903.47	6.0	750.82

377.91	139.03	918.75	5.14	751.02
864.51	463.49	908.97	5.64	752.02
474.46	834.39	918.36	9.13	752.03
47.0	419.1	937.15	4.59	752.07
850.12	374.51	923.51	5.29	752.11
240.92	501.66	928.1	4.3	752.41
954.91	496.53	915.09	5.8	753.04
145.86	307.09	961.5	4.82	754.54
589.92	317.41	927.65	5.12	756.33
242.91	523.47	928.24	6.15	756.6
523.98	572.82	928.87	6.12	757.77
222.06	849.95	928.13	362.94	757.88
192.97	661.03	941.39	5.92	758.59
381.35	619.92	949.61	6.31	758.82
327.44	30.94	938.56	363.83	759.22
186.43	137.48	943.28	363.8	760.23
632.5	936.41	929.89	6.7	760.31
789.56	621.56	929.87	404.21	761.02
909.36	211.37	932.14	7.27	761.24
215.93	314.0	941.87	420.88	762.19
142.3	358.39	941.32	364.95	762.96
366.5	895.55	935.52	420.5	763.54
880.42	149.03	944.73	6.38	763.58
377.34	952.75	1000.65	15.13	764.0
436.44	881.56	944.57	363.51	764.48
137.6	521.59	954.85	363.73	764.69
813.1	121.65	955.42	364.9	765.01
417.61	462.33	956.22	6.2	765.99
491.95	513.45	959.24	421.09	766.15
785.54	657.57	940.52	439.67	766.15
991.92	123.53	947.19	452.45	766.69
874.09	218.47	954.62	404.06	766.96
229.07	304.87	955.92	460.79	770.06
210.0	742.19	1037.72	4.44	770.16
523.57	604.0	961.51	464.09	771.97
878.0	373.5	970.73	437.34	772.02
219.84	982.85	954.12	461.35	772.49
55.93	982.02	991.18	7.28	772.65
233.49	960.85	963.21	455.07	772.84
406.61	67.13	968.5	450.08	773.04
833.04	709.97	951.7	465.68	773.1
676.06	405.85	962.16	461.79	773.48
256.92	491.71	971.92	463.36	775.51
834.57	6.66	982.21	435.39	776.91
541.99	376.94	978.53	464.7	777.03
378.01	103.15	978.06	461.05	777.49
804.03	241.43	982.94	461.47	777.8
511.03	105.07	1071.34	4.73	777.91
531.22	827.76	980.42	466.25	777.96
251.7	991.99	989.97	404.79	778.16
200.94	537.7	995.4	461.05	778.71
175.95	402.89	971.57	464.45	778.71
406.35	816.04	971.24	463.05	779.54
536.98	615.05	990.52	460.29	779.63
551.57	37.06	975.26	465.38	779.73
431.05	653.12	992.97	460.28	779.83
468.52	664.9	978.81	462.22	780.19
431.45	715.09	977.82	466.79	782.85

517.88	868.44	1025.59	450.15	783.54
349.48	340.91	992.55	466.13	784.12
207.43	229.63	994.67	466.89	785.12
106.56	625.67	1019.56	447.8	785.96
211.78	560.54	1015.12	466.24	787.32
208.08	100.42	1017.68	465.07	788.95
805.48	550.52	989.49	469.16	789.37
819.39	974.58	982.44	469.85	789.62
829.6	666.36	989.33	469.04	789.89
468.56	67.36	997.3	469.73	790.28
358.5	288.69	1008.62	468.86	791.7
245.82	299.43	1005.08	469.07	791.87
406.05	871.41	1003.82	470.22	792.69
492.92	406.57	1017.23	471.47	792.87
622.98	632.34	1000.48	470.61	793.4
339.59	103.49	1012.91	469.63	793.67
308.49	273.49	1006.91	470.68	794.38
909.92	514.94	1006.84	471.48	794.46
829.03	274.39	1009.18	470.39	794.47
792.89	307.5	1004.53	470.79	795.15
559.7	900.57	1157.11	5.36	795.54
728.52	163.42	1007.98	471.79	795.64
659.03	730.07	1008.3	470.42	796.01
483.25	817.45	1028.55	470.47	796.17
51.37	723.0	1014.59	468.97	796.42
947.1	710.55	1006.74	472.37	797.12
131.59	400.99	1081.05	471.11	798.05
222.79	544.21	1030.97	471.1	798.2
523.04	253.5	1029.95	469.86	798.64
168.61	697.53	1195.07	5.03	799.44
7.25	738.54	1026.15	457.13	799.78
261.36	552.94	1020.82	469.75	800.02
927.86	988.03	1010.5	472.59	800.53
418.26	507.1	1046.78	471.9	800.96
349.84	736.07	1048.75	472.25	802.93
385.56	565.47	1048.93	471.51	803.13
553.64	882.56	1133.37	459.92	803.49
773.92	369.43	1022.77	476.12	805.17
655.09	635.54	1022.82	453.15	805.34
488.94	29.04	1043.42	473.0	806.68
609.45	350.27	1062.0	476.27	806.68
378.62	711.44	1039.23	475.07	806.88
944.55	20.87	1072.49	471.68	808.82
463.51	100.08	1049.86	474.07	809.11
702.47	831.16	1028.29	475.95	809.2
655.04	126.7	1071.53	471.2	809.43
244.25	699.21	1108.03	471.58	811.34
582.54	22.01	1047.3	478.07	811.85
335.04	539.19	1092.89	471.26	812.77
965.79	676.22	1089.29	473.15	814.45
703.02	871.52	1047.92	477.82	816.27
480.16	206.79	1055.09	475.78	816.31
411.63	649.25	1064.72	477.43	816.35
306.07	755.98	1046.79	479.04	816.6
882.02	84.89	1103.55	470.66	816.63
486.19	535.46	1147.4	479.06	817.05
311.82	453.25	1061.86	478.73	817.61
949.13	571.62	1086.09	480.67	818.6

97.99	260.9	1146.69	468.9	818.86
45.27	939.48	1444.32	10.83	819.61
568.17	535.78	1217.18	459.6	819.89
427.08	137.93	1096.1	478.09	820.18
612.55	96.95	1064.53	480.04	821.54
252.08	407.89	1071.08	480.92	821.83
194.38	904.85	1111.29	473.2	822.71
175.38	346.55	1084.2	479.46	824.98
1003.58	302.0	1069.2	484.11	825.32
479.38	297.17	1081.89	483.29	826.19
863.98	575.57	1067.93	484.14	826.86
410.87	689.0	1077.52	482.16	827.29
915.65	153.62	1126.52	477.21	829.31
637.97	461.15	1097.93	479.99	830.24
265.47	939.82	1097.78	475.89	832.66
324.76	466.27	1089.3	485.79	833.35
634.97	575.5	1098.36	484.62	833.56
584.28	551.22	1105.61	483.3	833.77
1014.68	10.08	1106.48	485.14	834.03
579.49	442.5	1126.56	481.3	836.02
364.24	752.25	1098.37	486.08	836.37
510.29	892.19	1107.53	484.58	836.37
766.65	649.33	1085.12	487.33	837.03
170.37	242.47	1095.7	486.61	837.76
770.54	572.01	1088.22	486.71	838.1
671.45	617.37	1090.86	487.41	838.41
1015.37	583.5	1089.98	490.0	839.42
657.0	806.05	1110.1	486.08	840.64
289.45	641.39	1112.77	488.05	842.41
745.48	866.47	1098.3	486.76	842.67
838.11	611.62	1106.7	486.9	842.7
72.01	231.78	1116.98	489.24	842.77
549.06	353.09	1121.31	486.45	843.56
877.0	305.0	1277.7	468.23	844.93
939.54	424.59	1111.94	487.98	846.78
322.98	969.35	1115.51	488.69	847.17
538.44	197.34	1127.58	488.9	848.82
166.5	92.32	1147.35	484.07	849.93
49.27	920.73	1154.73	484.11	850.96
93.48	667.61	1276.57	469.32	851.63
309.03	658.42	1138.93	500.03	852.1
533.08	655.71	1153.57	490.1	854.37
179.38	532.45	1241.99	483.56	856.43
313.28	528.0	1159.73	492.41	858.29
410.05	268.04	1140.0	494.17	859.57
781.47	506.44	1146.31	495.64	861.45
488.46	468.32	1179.99	493.45	862.68
693.98	124.47	1161.17	490.85	862.69
544.84	923.61	1179.77	490.26	863.54
616.1	233.58	1160.2	495.16	865.29
244.23	945.27	1195.45	490.76	867.35
584.0	107.65	1171.04	495.93	869.86
388.26	407.0	1174.96	498.76	871.05
177.89	479.5	1182.3	501.8	873.99
649.44	558.26	1210.15	497.1	877.05
208.4	63.38	1233.11	490.71	877.66
628.97	282.19	1174.3	502.07	879.23
757.17	738.03	1171.11	502.55	879.6

465.72	446.98	1225.77	502.82	882.17
876.53	837.89	1198.12	504.72	888.06
100.56	439.4	1224.1	511.69	890.66
611.69	756.14	1257.33	503.39	894.06
992.44	692.11	1191.25	510.9	894.62
402.38	773.96	1220.17	506.83	897.43
652.38	991.04	1258.13	501.63	897.73
623.12	132.74	1249.15	510.8	904.76
293.87	549.73	1318.81	507.48	905.19
501.01	715.03	1270.97	507.48	905.92
470.33	237.08	1257.8	506.5	907.05
989.31	770.93	1272.09	506.7	909.58
140.94	636.11	1286.98	506.13	912.03
929.4	192.94	1279.41	508.57	914.75
701.46	704.92	1248.58	516.02	916.24
895.94	406.88	1271.23	515.13	917.83
174.36	321.83	1278.51	514.79	919.63
600.41	593.04	1286.29	514.8	920.62
375.45	454.82	1314.82	511.49	921.81
57.48	247.28	1864.77	467.72	924.79
283.57	234.84	1276.05	521.51	929.62
214.81	519.85	1310.44	517.39	930.37
930.2	688.14	1312.18	519.34	932.73
189.9	202.88	1366.98	512.76	934.68
472.84	352.68	1119.67	527.18	936.15
725.6	265.46	1333.39	517.66	938.29
577.73	718.89	1361.94	513.3	939.13
664.07	472.12	1331.69	521.87	941.13
240.91	208.93	1316.84	522.6	941.69
827.68	158.57	1333.49	521.31	942.49
533.39	292.58	1321.52	523.47	943.21
583.21	367.21	1379.75	521.17	944.62
945.42	673.2	1346.46	524.1	945.68
96.05	410.36	1350.69	521.42	945.85
636.72	22.06	1326.55	523.13	946.53
347.38	695.65	1348.48	525.4	947.78
876.54	795.53	1778.34	482.98	949.69
592.41	765.49	1360.47	525.29	950.33
499.18	294.48	1359.94	524.15	954.03
697.06	459.13	1353.22	527.17	955.36
316.61	428.15	1408.2	517.42	958.84
349.33	364.37	1442.69	533.69	976.0
784.33	486.36	1394.38	539.63	982.39
402.42	207.97	1406.9	540.29	983.53
668.7	352.2	1696.6	505.7	993.07
278.89	305.63	1424.98	543.93	994.81
455.01	695.21	1491.89	547.82	1013.41
314.05	610.45	1491.41	547.27	1014.68
534.66	747.63	1535.11	539.47	1015.22
479.16	418.76	1518.61	550.32	1019.51
272.06	592.25	1590.43	549.46	1038.5
863.56	781.61	1688.05	532.84	1042.16
483.23	189.97	1558.82	557.07	1043.04
816.19	725.23	1547.24	561.09	1049.88
622.33	773.43	1656.67	547.3	1053.06
437.71	539.23	1814.21	553.36	1055.29
688.5	671.61	1556.88	571.0	1060.25
388.97	670.93	1620.17	565.83	1067.53

965.84	579.1	1588.72	570.92	1069.26
213.57	427.31	1721.05	561.88	1090.7
426.92	628.09	1856.36	619.33	1092.65
447.38	437.03	1727.01	579.5	1109.14
501.27	831.31	1827.04	565.49	1112.11
256.55	630.84	1783.53	571.8	1114.5
759.69	434.11	1703.73	584.32	1116.04
179.56	560.57	1724.34	569.53	1123.27
34.99	195.0	1717.77	588.96	1125.56
276.08	414.36	1742.07	603.33	1142.4
576.72	477.01	1868.27	592.44	1165.22
391.13	472.38	1810.42	609.37	1174.64
215.36	657.46	1964.89	592.76	1185.41
333.55	726.22	1922.96	617.47	1206.96
208.45	258.46	1905.68	630.9	1230.18
576.34	246.38	1877.06	625.33	1239.83
342.28	240.54	2072.77	645.47	1292.12
348.46	606.17	2157.93	645.7	1308.91
678.34	266.51	2174.71	647.82	1323.31
699.05	209.89	2236.2	643.86	1346.55
211.61	203.04	2236.57	661.04	1351.53
463.98	537.9	2344.18	698.87	1374.9
675.61	193.23	2373.69	669.59	1385.68
224.48	697.41	2281.63	701.29	1403.19
182.45	757.79	2285.21	675.26	1412.1
135.35	13.9	2405.51	683.57	1412.46
1003.93	32.21	2487.13	671.26	1427.45
375.9	519.77	2352.73	696.51	1431.68
750.39	457.76	2430.15	685.73	1432.8
589.39	345.87	3483.85	573.88	1436.2
895.92	670.32	2527.18	673.45	1439.73
336.32	146.35	2437.48	689.39	1446.97
232.05	442.04	2408.26	705.63	1449.51
272.9	618.75	2406.46	720.45	1451.49
327.52	918.67	2752.01	698.7	1527.14
296.02	948.38	2759.68	719.77	1557.84
354.28	471.02	2583.45	773.17	1578.3
540.17	506.22	3080.11	758.85	1616.78
425.53	156.52	2778.68	762.06	1617.55
588.93	946.8	3188.54	759.23	1720.07
419.67	384.45	3153.57	824.32	1780.73
180.55	613.45	3361.48	816.11	1809.54
359.18	940.13	4930.4	668.64	1910.39
993.74	416.88	3445.05	857.98	1910.91
426.53	360.08	3731.27	866.05	1982.9
361.43	843.87	4155.42	880.81	2115.84
240.16	577.92	4197.34	926.41	2170.08
261.87	672.39	4324.22	993.48	2299.86
125.17	577.5	4484.12	972.22	2305.62
442.09	558.01	5285.58	1120.74	2653.73
132.78	418.45	5182.61	1148.23	2708.04
78.93	161.89	5569.32	1149.3	2799.07

Appendix C: Measured Fluxes of Wild Duck

X (pix)	Y (pix)	R Flux	B Flux	V Flux
290.5	1021.27	13.97	1.36	6.42
87.5	1017.97	20.99	2.22	7.12
1021.95	746.19	22.47	1.61	7.93
440.3	569.62	18.85	15.11	8.62
895.91	987.06	31.76	2.96	8.7
1022.81	19.54	279.9	1.17	9.12
392.13	636.57	21.58	1.78	9.16
307.24	671.44	19.98	2.15	9.34
216.89	416.02	30.06	173.88	9.58
4.03	768.33	22.04	1.87	9.71
931.82	519.89	22.25	2.08	9.72
731.36	299.07	26.49	1.73	9.76
258.47	575.24	22.27	2.24	9.82
350.48	324.95	24.56	1.97	9.92
10.39	793.38	24.04	2.14	9.97
319.35	250.76	22.69	2.18	10.12
147.21	825.13	23.4	2.51	10.33
612.17	646.13	23.42	2.06	10.38
383.3	990.49	27.9	2.21	10.39
633.15	696.2	23.76	2.26	10.44
813.66	416.45	22.47	2.15	10.47
966.06	128.65	26.87	2.17	10.51
609.79	374.82	24.63	2.11	10.58
654.28	958.91	24.82	2.39	10.59
436.5	113.54	23.94	2.22	10.64
613.89	260.8	22.56	2.24	10.67
389.56	581.33	348.15	7.86	10.7
1.13	340.18	27.41	2.04	10.72
166.37	979.07	27.01	2.25	10.8
339.84	383.68	24.72	2.65	10.86
779.5	882.6	23.89	2.03	11.07
484.72	1003.6	26.08	2.29	11.11
83.68	979.91	28.1	2.26	11.12
453.94	404.68	24.34	2.34	11.2
14.8	656.74	31.92	1.86	11.25
819.03	662.99	26.68	2.32	11.26
577.99	199.98	25.96	1.94	11.28
425.98	326.0	26.6	1.99	11.35
35.21	308.93	26.42	2.51	11.36
808.41	812.97	21.06	2.31	11.39
860.32	276.91	26.21	2.09	11.42
401.29	849.72	25.22	2.25	11.43
697.58	506.07	30.6	6.74	11.46
605.01	239.03	35.74	2.25	11.6
364.04	674.06	29.51	2.02	11.71
372.46	306.6	30.51	2.26	11.71
868.96	830.95	28.04	2.23	11.8
552.54	958.18	30.52	1.88	11.81
655.45	1016.12	24.66	2.27	11.87
347.31	80.1	30.33	2.31	11.89
726.1	332.13	26.03	2.64	11.95
879.07	656.86	27.56	2.25	11.98
688.71	667.89	24.06	2.16	11.98
704.84	1019.93	30.61	2.02	11.99

417.29	366.3	33.35	1.91	12.03
141.45	630.71	29.04	2.37	12.07
676.05	566.77	26.33	2.9	12.16
67.94	317.13	32.18	2.4	12.31
254.99	698.03	29.57	2.34	12.38
905.18	412.9	28.78	2.48	12.38
321.16	274.86	31.35	2.76	12.42
550.09	175.99	26.34	2.69	12.44
747.61	43.9	32.04	2.62	12.52
144.18	248.82	27.37	2.79	12.52
652.97	208.24	29.83	2.26	12.55
987.9	520.38	27.17	2.35	12.6
447.16	712.99	26.51	2.61	12.65
1014.49	479.09	31.89	3.25	12.65
1005.28	30.09	28.73	2.53	12.75
479.91	278.03	27.36	2.73	12.75
792.18	363.37	274.64	3.16	12.76
286.98	278.46	32.33	3.18	12.8
584.86	646.82	348.71	3.2	12.88
773.17	112.63	30.77	2.09	12.89
447.33	346.01	34.3	2.9	12.91
602.63	793.22	30.22	1.79	12.92
858.48	753.07	30.58	4.01	12.92
256.88	836.04	28.95	2.55	12.92
526.4	108.09	29.91	2.22	12.94
86.86	719.1	32.26	2.12	12.98
362.91	470.9	28.55	4.15	13.08
474.85	64.38	27.72	2.49	13.14
176.68	809.34	33.46	2.26	13.18
270.16	362.66	32.67	2.82	13.3
305.95	821.69	35.25	2.6	13.31
477.01	760.68	347.97	1.99	13.4
531.22	373.38	30.02	3.03	13.62
172.63	717.18	34.04	2.07	13.68
750.48	503.38	31.28	3.26	13.7
518.96	377.42	31.86	2.86	13.78
665.62	843.4	28.55	3.22	13.84
449.11	294.67	33.27	5.84	13.86
340.24	295.53	31.89	2.51	14.06
802.98	658.62	345.7	2.64	14.08
764.31	654.65	31.08	3.06	14.08
644.24	274.26	33.7	2.57	14.09
180.67	963.17	30.84	2.2	14.14
499.88	600.29	30.33	2.92	14.16
97.81	99.82	34.15	3.36	14.18
926.77	397.82	38.37	2.58	14.28
932.34	13.13	29.69	3.19	14.33
888.12	965.61	34.03	3.4	14.39
396.11	595.41	363.89	2.06	14.41
384.99	355.39	28.92	3.07	14.44
21.56	131.21	40.09	2.36	14.45
924.1	912.01	342.64	3.07	14.48
868.44	176.95	34.35	3.02	14.52
1015.95	554.85	344.66	2.3	14.53
103.07	389.19	29.6	3.46	14.54
420.09	220.35	32.06	3.34	14.74
19.49	882.75	37.06	2.77	14.79
979.31	441.94	349.16	3.64	14.81

452.48	802.51	32.18	3.08	14.92
159.01	206.39	33.99	3.25	14.94
384.13	747.6	29.85	3.37	14.97
899.81	281.64	37.21	2.61	15.03
91.71	326.34	349.64	1.96	15.05
257.6	484.22	35.74	3.12	15.06
151.54	818.0	31.85	3.45	15.11
595.87	846.84	33.82	2.83	15.31
940.51	921.99	341.53	2.97	15.31
144.51	770.98	339.59	3.31	15.35
653.56	378.38	48.1	2.01	15.41
50.48	203.56	37.66	2.69	15.47
722.53	60.41	35.44	3.78	15.49
324.23	231.52	336.68	2.75	15.63
384.4	831.44	349.6	2.43	15.7
244.89	697.82	35.65	3.37	15.72
162.84	792.21	344.22	3.14	15.76
634.21	512.32	347.4	3.24	15.77
364.4	354.27	33.31	3.88	15.81
671.43	898.33	343.34	3.83	15.98
352.09	440.98	334.16	3.58	16.12
985.23	458.76	344.67	3.33	16.13
111.69	754.26	33.61	3.57	16.27
215.83	961.32	39.22	3.35	16.33
838.69	210.52	340.25	3.11	16.34
912.35	799.95	343.94	9.15	16.36
690.89	714.64	343.06	3.88	16.44
733.21	357.76	338.7	9.55	16.47
953.32	652.99	342.12	3.23	16.58
470.19	229.5	37.22	3.41	16.58
295.47	621.61	35.98	3.88	16.6
878.11	165.28	337.18	3.49	16.68
645.89	39.67	339.67	3.69	16.69
815.77	538.63	32.97	3.69	16.69
276.18	589.27	339.87	3.24	16.71
398.16	32.22	337.99	3.14	16.72
933.06	739.81	341.11	3.71	16.94
564.92	811.24	361.96	2.81	16.98
858.43	240.45	34.74	3.48	17.0
1018.32	192.82	355.17	2.56	17.02
74.19	209.02	360.21	2.43	17.2
840.3	374.88	349.63	3.11	17.22
1018.96	208.66	343.36	3.42	17.24
643.04	675.65	347.62	3.28	17.45
581.16	114.38	42.19	3.37	17.58
1006.81	620.89	345.53	3.96	17.71
709.43	825.56	39.08	4.11	17.73
597.25	634.27	345.57	3.65	17.75
348.27	914.34	37.92	4.0	17.83
25.69	831.49	344.05	3.33	17.91
671.54	754.23	350.06	4.2	18.11
715.01	8.19	369.61	1.88	18.23
697.4	113.1	34.56	175.5	18.28
927.3	46.77	337.72	4.29	18.3
309.2	521.45	343.23	3.93	18.33
607.65	175.75	342.31	4.06	18.39
91.39	815.29	354.71	3.41	18.42
372.39	741.83	366.79	3.6	18.42

925.02	382.96	343.74	3.9	18.52
232.73	192.85	365.6	2.36	18.52
912.18	981.47	345.7	4.07	18.54
834.67	917.44	370.31	2.07	18.56
134.74	837.16	346.46	3.9	18.58
71.57	165.61	42.33	4.13	18.72
693.67	321.88	339.63	3.82	18.75
148.31	848.31	340.95	4.06	18.85
500.64	706.58	349.63	3.96	19.03
177.46	147.11	337.06	4.64	19.14
511.08	196.27	346.98	4.37	19.2
911.41	889.39	381.19	1.95	19.21
266.43	882.35	377.21	2.1	19.92
673.45	483.84	362.42	4.13	20.22
1005.95	116.71	363.15	2.06	20.34
25.59	348.4	337.99	4.38	20.62
33.13	134.91	354.66	4.2	20.82
112.44	135.69	360.67	3.67	22.0
109.36	653.5	346.63	5.27	22.38
69.58	656.89	356.49	5.57	23.68
9.43	260.81	341.2	4.5	268.4
505.07	139.07	343.95	4.22	269.48
482.04	389.97	343.81	4.49	270.15
330.28	523.6	376.67	20.8	270.16
481.51	372.0	344.53	5.48	270.5
29.92	213.01	342.86	5.46	271.06
670.98	88.93	357.95	3.84	271.25
328.99	503.49	347.16	4.75	271.32
91.97	493.96	347.31	174.91	271.78
141.74	677.33	345.82	5.24	271.83
40.47	880.21	376.69	3.56	272.17
215.02	225.91	349.74	6.07	272.23
75.96	195.96	355.06	4.7	272.26
585.09	56.98	384.39	2.99	272.36
29.35	787.0	351.85	5.37	272.64
508.17	343.79	349.53	5.34	272.73
183.02	382.01	349.04	175.55	272.73
482.99	155.91	353.65	5.12	272.8
83.99	767.09	383.66	2.59	272.91
34.95	22.53	390.86	3.08	272.92
297.29	12.47	352.3	5.05	272.93
691.0	29.92	349.07	5.25	272.95
591.86	419.88	360.42	3.45	272.99
383.04	275.46	348.8	5.63	273.19
302.0	738.0	354.53	4.89	273.58
506.98	784.47	349.79	4.41	273.67
545.85	300.97	355.95	4.91	273.8
480.04	505.05	350.38	5.58	273.83
89.96	238.03	384.05	3.15	273.86
84.98	313.0	356.92	175.06	274.03
148.98	667.11	400.2	2.16	274.26
851.01	192.99	364.71	4.01	274.35
517.04	393.03	353.06	176.17	274.45
243.96	153.96	425.38	2.33	274.55
432.01	1007.91	380.97	2.65	274.87
407.93	797.0	357.93	5.02	274.88
162.31	432.25	357.11	175.42	274.92
31.87	868.86	354.76	176.16	274.97

511.51	809.99	351.46	5.12	275.09
260.99	744.92	367.31	4.49	275.23
659.47	261.04	356.89	176.18	275.26
170.5	94.0	356.19	175.36	275.57
823.22	743.89	361.75	8.17	275.57
951.04	512.97	379.01	3.07	275.66
546.54	431.97	359.35	176.14	275.82
210.47	579.05	401.18	2.17	275.95
642.39	626.07	356.26	8.94	275.96
418.14	396.71	361.81	7.79	276.02
497.03	444.42	356.55	177.15	276.08
1018.03	420.5	361.29	3.05	276.29
30.62	412.64	356.65	176.08	276.43
372.03	595.56	356.74	177.12	276.55
200.04	968.46	356.27	177.01	276.74
95.57	954.56	353.68	176.61	276.87
103.43	841.0	389.51	3.22	276.91
438.0	796.06	368.0	4.22	276.98
802.05	884.95	353.84	177.67	277.14
47.69	683.65	398.41	13.19	277.24
776.02	833.32	370.39	18.89	277.3
7.96	895.46	373.25	4.89	277.51
646.49	799.5	389.88	2.85	277.75
200.53	371.46	358.84	176.45	277.78
982.43	740.44	369.71	3.96	277.83
390.01	937.0	359.12	177.66	277.9
301.0	834.99	356.26	177.24	278.08
545.38	806.0	361.09	4.95	278.17
432.0	693.43	359.79	177.3	278.19
545.66	710.85	359.87	176.97	278.2
311.01	723.33	359.75	177.63	278.49
467.53	561.43	359.28	177.44	278.53
3.29	252.05	395.79	3.75	278.77
331.04	798.06	362.31	177.54	278.8
923.49	273.98	356.59	177.59	278.85
771.6	595.5	358.0	177.47	278.89
50.56	598.57	371.72	176.1	279.04
57.05	653.61	364.88	176.37	279.07
687.49	385.08	360.53	177.62	279.11
800.43	443.52	370.93	4.82	279.44
374.42	614.0	363.78	176.83	279.65
362.42	940.51	364.88	177.14	279.7
559.55	775.0	362.75	180.2	279.77
246.47	452.54	362.51	177.34	279.77
680.54	920.03	363.76	5.76	279.8
5.49	827.51	406.67	3.22	280.02
787.0	727.0	365.0	177.74	280.03
757.85	519.75	360.28	177.9	280.07
260.47	531.39	363.93	177.09	280.14
903.46	599.53	361.62	178.19	280.31
745.42	997.5	367.07	177.49	280.37
344.74	1005.91	401.29	117.83	280.54
439.58	376.43	366.73	177.44	280.58
825.51	567.04	358.35	178.77	280.65
898.96	718.47	363.03	177.97	280.74
749.79	530.78	365.69	177.78	281.02
421.32	747.37	364.79	178.57	281.18
708.81	449.36	365.31	178.17	281.6

869.55	362.45	365.47	178.44	281.64
849.01	829.49	364.49	178.67	281.82
332.52	736.51	369.59	177.82	281.87
893.46	696.28	350.76	178.97	281.99
191.54	931.84	416.27	3.82	282.0
794.62	902.39	407.8	3.2	282.01
371.44	183.37	367.57	177.12	282.03
953.54	564.46	365.73	178.67	282.17
609.54	301.46	366.76	177.93	282.21
692.01	416.07	363.2	178.55	282.21
9.49	555.44	371.55	177.24	282.28
468.42	737.5	362.79	178.58	282.29
877.45	101.52	382.06	5.43	282.38
694.46	224.46	369.95	176.99	282.39
826.93	116.44	364.62	177.66	282.45
393.6	529.53	371.8	178.84	282.51
468.47	397.54	370.45	177.92	282.53
492.54	772.45	366.0	178.66	282.59
865.58	571.5	369.36	178.45	282.68
903.46	384.54	379.44	5.12	282.85
130.58	436.52	372.31	177.77	282.86
492.1	403.98	368.83	179.13	282.86
763.0	554.5	386.09	4.91	282.89
385.27	665.13	382.25	178.93	282.91
363.51	812.59	378.4	177.51	283.1
880.97	578.4	415.9	3.16	283.12
464.05	914.95	409.5	2.88	283.13
531.03	403.54	377.29	178.03	283.24
781.04	411.5	417.08	2.82	283.25
403.0	273.01	369.45	178.11	283.28
299.55	604.46	372.26	178.06	283.43
125.61	930.79	384.67	176.6	283.43
838.54	351.53	370.68	177.98	283.5
694.6	486.03	371.19	178.66	283.57
366.5	633.51	370.43	179.0	283.73
715.08	681.58	374.72	178.85	283.76
417.47	272.97	370.09	178.23	283.96
673.02	739.63	375.69	178.78	284.02
632.5	813.5	413.77	3.15	284.32
398.98	348.47	419.54	3.47	284.54
56.43	98.07	371.71	178.8	284.61
376.53	341.56	387.0	177.07	284.7
392.0	442.51	377.16	178.36	284.73
792.55	122.53	370.27	178.12	284.83
481.53	565.58	376.1	178.89	284.83
654.58	780.51	388.25	177.59	284.88
1007.5	755.45	374.7	178.83	285.11
204.53	64.54	398.35	175.99	285.55
867.53	960.03	419.91	3.57	285.63
435.23	467.29	350.4	179.36	285.65
399.54	506.53	375.38	178.69	286.02
352.14	270.16	435.33	5.01	286.09
511.39	438.89	383.04	179.08	286.34
464.1	755.51	372.15	179.4	286.48
974.93	471.94	409.48	4.61	286.69
671.93	935.51	371.96	179.9	286.71
611.08	605.61	374.13	179.77	286.73
378.03	377.46	374.31	180.43	286.73

873.94	67.93	373.44	178.57	286.84
723.01	217.98	376.73	179.03	287.01
438.58	558.01	378.6	179.34	287.01
810.17	465.99	376.87	179.66	287.02
410.94	55.94	382.03	178.06	287.2
888.9	499.97	376.78	179.38	287.49
252.09	925.07	401.46	177.33	287.69
584.96	378.41	378.65	179.97	287.86
62.51	923.91	397.72	177.38	287.86
128.89	493.97	438.43	4.01	287.91
136.94	926.68	420.33	16.25	288.34
352.07	562.2	376.46	180.25	288.84
164.97	346.89	465.2	4.0	288.84
585.11	576.89	376.4	180.46	288.93
108.53	326.96	396.32	177.2	288.99
356.72	796.78	384.49	179.81	289.04
238.02	747.02	378.52	180.37	289.16
314.77	558.83	386.76	180.47	289.41
99.95	667.92	392.78	179.19	289.62
927.53	672.97	407.34	177.66	289.72
668.98	196.97	378.68	180.42	289.88
275.95	604.5	383.35	180.37	290.07
675.94	606.42	404.31	178.37	290.16
617.08	318.86	408.43	177.52	290.18
445.53	868.06	380.67	180.24	290.19
279.98	313.48	383.08	179.99	290.27
382.97	478.96	386.73	179.99	290.79
885.96	430.98	400.14	178.68	290.86
299.05	70.88	410.07	177.76	290.98
916.89	862.11	465.85	3.02	291.16
414.18	423.43	385.37	180.53	291.24
897.01	770.95	404.69	178.38	291.27
925.87	131.0	432.27	4.69	291.45
513.02	984.03	381.56	180.94	291.47
213.52	643.02	385.98	180.27	291.7
112.66	582.1	449.16	6.14	291.72
149.52	481.36	401.96	180.2	291.73
724.12	546.13	383.36	181.16	291.8
224.06	976.02	444.72	4.42	291.84
337.08	362.87	389.0	180.58	292.06
662.86	348.67	436.02	176.75	292.16
239.08	856.07	386.93	181.15	292.22
61.99	838.99	687.38	3.55	292.34
561.46	787.18	383.44	180.77	292.41
308.29	622.15	386.53	181.25	292.7
751.96	147.04	401.13	179.52	292.9
558.01	715.71	391.96	181.42	293.2
565.05	600.58	404.33	184.85	293.78
573.81	224.27	388.79	180.88	293.88
964.97	168.07	389.39	180.25	293.9
304.87	634.69	389.14	181.3	293.93
975.0	967.01	399.57	179.99	294.11
762.99	932.99	387.76	181.0	294.15
155.71	879.66	444.57	4.61	294.32
463.75	655.9	429.06	187.45	294.32
399.61	537.74	392.36	182.22	294.32
341.81	281.26	392.81	180.41	294.33
156.1	943.9	391.83	181.79	294.96

734.96	585.75	404.87	180.56	294.98
589.15	560.95	391.94	181.48	295.36
827.06	309.07	391.42	180.87	295.37
787.9	992.97	393.01	182.37	295.68
795.09	468.49	391.5	181.66	295.99
593.44	659.5	390.5	182.31	296.06
523.72	455.36	398.03	183.97	296.2
282.23	380.68	394.57	181.73	296.48
654.47	981.48	389.06	182.19	296.86
205.36	666.03	402.08	182.02	297.06
841.41	664.01	401.74	182.14	297.24
656.94	703.94	395.98	182.63	297.37
823.1	807.09	464.36	4.53	297.53
364.98	142.03	430.17	177.7	297.55
832.43	425.57	403.04	181.08	297.56
659.0	758.0	400.68	181.7	297.71
547.56	602.14	395.5	183.81	297.82
426.43	851.11	398.7	182.96	297.91
3.81	19.18	486.81	150.89	298.14
489.35	584.63	399.38	182.48	299.0
373.05	236.96	404.94	181.8	299.13
649.95	926.03	396.41	183.07	299.23
165.19	892.18	438.5	179.03	299.38
478.69	646.23	404.66	181.78	299.8
807.03	511.97	406.64	182.91	300.25
1011.99	525.99	403.21	182.92	300.57
345.53	842.63	395.85	183.09	300.98
463.28	599.54	403.24	183.64	301.01
650.09	337.85	402.72	183.02	301.12
864.96	456.97	412.86	182.3	301.57
152.63	620.0	488.29	5.2	302.53
1011.37	460.55	425.64	181.5	302.87
576.53	556.68	409.05	183.56	303.2
73.96	885.48	436.25	180.5	303.44
191.47	448.54	450.08	181.15	303.52
538.35	594.09	414.14	183.21	303.62
404.28	902.79	404.93	184.45	303.75
713.55	630.04	412.08	184.0	303.91
515.04	739.3	409.71	184.64	303.93
146.95	728.44	557.41	4.43	304.08
446.35	822.62	411.84	184.34	304.4
55.46	460.59	484.62	176.47	304.56
559.82	933.79	402.62	185.56	305.05
365.52	695.51	409.67	184.3	305.06
434.88	836.7	411.25	184.46	305.24
506.52	421.58	415.17	183.81	305.41
513.87	633.74	412.22	187.84	305.64
626.84	546.3	410.09	186.72	305.74
452.93	742.31	414.08	183.75	305.91
443.98	881.44	412.42	185.29	306.11
687.0	774.0	422.88	184.21	306.29
873.79	755.03	408.61	184.73	306.87
489.91	306.12	492.17	177.27	307.23
329.19	592.7	410.59	186.13	307.49
764.4	356.9	426.93	182.88	307.69
341.46	774.38	422.13	185.21	307.83
678.15	539.68	426.21	184.83	308.12
966.59	765.53	416.04	185.74	309.06

390.37	699.84	537.73	15.99	309.15
527.79	442.58	424.71	185.76	309.64
710.81	379.58	440.96	182.48	309.68
842.04	400.52	422.65	186.15	310.56
484.88	692.38	431.17	187.12	310.59
216.55	436.05	426.63	184.66	310.66
522.31	510.62	428.03	190.5	310.78
611.42	354.88	400.1	185.21	310.81
778.66	820.61	422.73	186.16	310.86
500.71	577.28	424.17	185.11	311.17
665.29	659.15	515.82	181.49	311.34
733.55	17.46	438.13	182.18	312.2
419.99	678.56	426.55	186.93	312.26
318.27	787.43	426.87	185.97	312.69
362.98	510.26	438.15	186.81	313.19
849.53	545.52	529.34	177.98	313.28
810.16	748.79	426.72	187.39	313.32
350.06	233.12	433.53	185.27	313.47
820.52	721.65	596.16	4.47	313.51
637.6	525.16	432.67	186.61	314.22
474.2	608.0	433.87	188.74	314.82
976.6	855.47	441.25	185.16	314.82
838.5	882.39	428.12	187.26	314.96
415.35	584.44	431.25	186.45	315.1
721.59	975.53	440.78	185.02	315.51
618.7	667.85	431.63	187.03	315.86
347.59	609.83	419.66	189.76	316.81
564.84	233.47	442.81	185.92	317.0
301.75	474.9	420.16	186.58	317.11
355.38	743.51	546.64	177.53	317.82
627.55	482.22	432.63	189.02	318.25
869.12	741.26	435.93	187.65	318.32
456.71	679.79	453.83	184.77	318.35
7.37	175.45	436.42	188.29	319.14
436.57	291.36	440.71	186.77	319.32
671.69	520.2	483.54	184.88	319.4
17.57	810.5	440.19	187.88	319.62
653.4	403.47	442.86	187.6	320.13
215.45	766.99	517.5	179.82	320.24
925.44	803.44	440.45	188.41	320.71
21.63	520.67	454.44	188.01	320.97
668.61	446.07	445.82	188.4	321.17
503.32	356.93	444.34	188.2	321.29
43.67	790.59	543.45	178.52	321.33
35.07	677.25	445.1	188.62	321.55
661.22	554.08	450.47	191.27	322.44
678.18	682.5	461.72	185.55	322.48
607.94	667.07	446.38	188.52	322.55
460.73	166.22	461.64	187.51	323.23
248.59	614.53	539.95	179.85	323.26
564.57	321.88	449.19	188.62	324.05
352.13	1013.47	464.96	187.93	324.3
379.41	546.61	549.95	178.96	324.62
385.56	774.57	445.6	190.43	324.7
614.4	441.36	448.98	190.41	325.03
533.24	501.32	456.83	189.43	325.62
860.51	779.43	533.7	180.59	325.68
113.1	817.16	574.05	178.57	326.28

111.83	938.56	553.9	179.41	326.32
271.16	391.31	462.93	188.12	326.35
294.45	988.06	544.5	180.11	326.42
283.75	486.8	452.81	189.87	326.64
752.0	705.66	459.61	198.19	327.31
534.22	740.53	461.09	191.26	327.46
357.76	396.01	471.23	196.92	327.49
576.17	523.48	518.44	189.39	329.27
488.23	536.71	469.26	190.3	330.6
445.95	75.91	465.42	189.83	331.06
681.56	468.05	469.55	191.62	331.89
527.73	661.83	458.66	191.43	332.62
715.87	899.41	586.06	180.3	332.95
453.45	576.09	470.46	190.16	333.1
54.53	504.1	479.52	190.17	333.42
378.17	510.2	465.84	191.28	333.93
658.09	155.45	467.83	191.14	335.19
247.84	545.7	475.75	202.11	336.69
570.52	396.08	468.69	192.15	336.97
75.46	695.55	522.68	186.0	336.99
713.62	951.91	467.53	192.64	337.85
493.51	669.56	472.82	193.69	337.99
495.22	200.49	481.55	192.1	338.41
608.12	912.9	509.07	189.96	338.55
275.97	104.53	488.56	190.74	338.57
875.14	606.92	471.98	193.78	339.55
554.55	726.57	492.64	193.76	340.24
312.5	308.0	485.34	192.83	341.06
661.67	644.16	488.09	195.99	341.84
660.92	581.56	489.62	193.28	341.89
218.06	596.5	491.15	192.91	342.2
646.52	463.96	478.89	194.35	342.46
439.65	415.52	486.94	193.46	342.7
354.46	482.33	483.75	194.08	342.93
392.76	890.8	629.92	181.83	342.99
858.01	617.85	710.44	178.34	343.35
836.72	569.64	515.23	193.6	344.22
534.88	754.44	499.3	198.39	346.31
824.94	512.12	492.35	195.43	347.25
501.66	656.49	496.92	194.46	347.9
530.14	585.8	501.62	195.68	351.28
762.65	694.2	585.49	190.35	351.36
728.1	666.13	503.17	196.06	352.09
725.21	690.6	523.6	195.64	352.98
706.0	703.88	520.9	195.49	353.18
568.04	507.6	513.91	197.72	354.38
8.04	386.09	549.96	191.44	354.42
685.13	276.11	512.81	195.39	355.2
570.06	733.13	537.12	196.34	355.39
312.24	13.21	513.02	196.48	356.7
452.43	693.1	523.36	198.17	356.8
397.06	116.06	560.69	191.06	357.11
293.87	754.07	506.35	199.0	357.58
624.17	682.26	530.78	197.43	360.92
503.37	642.01	591.28	204.31	361.19
656.52	522.31	525.74	199.13	361.99
399.2	314.17	528.95	197.85	362.17
459.93	447.98	561.58	200.95	362.86

824.95	695.07	679.14	183.83	363.06
440.46	671.94	528.81	199.68	363.61
171.47	446.61	539.29	198.57	363.82
539.94	276.05	543.1	196.66	364.96
731.1	72.95	529.89	196.61	365.0
805.8	682.98	531.2	199.6	365.04
694.49	443.34	530.5	199.68	365.23
785.97	143.11	523.33	199.28	365.54
564.04	433.99	530.41	199.99	365.58
654.51	359.22	530.84	199.07	365.74
318.81	588.3	526.32	202.83	366.26
418.92	410.3	538.83	200.43	366.36
961.11	591.97	731.04	183.27	366.55
590.69	685.03	545.64	199.82	367.26
648.9	535.95	527.7	202.65	368.24
935.95	783.55	536.55	199.79	368.71
677.09	322.42	538.91	200.88	369.07
476.92	324.0	540.94	201.82	369.27
557.8	654.64	502.51	203.81	369.27
630.41	663.67	553.78	201.89	369.92
577.82	769.76	550.11	200.31	370.26
435.37	403.3	568.94	199.73	371.25
623.46	592.7	544.38	201.09	371.28
957.07	683.55	689.59	186.41	372.44
598.47	347.76	552.55	201.96	373.99
524.07	699.94	553.25	200.5	374.03
498.1	491.22	543.96	206.59	374.19
260.88	551.39	560.09	203.41	375.37
370.28	526.84	551.18	203.4	376.11
651.18	313.02	556.3	202.23	376.94
695.48	559.6	566.69	202.44	378.86
470.74	934.94	557.94	206.2	378.88
533.78	607.94	560.53	202.4	379.37
608.72	559.45	561.31	206.58	381.37
558.9	570.56	564.57	202.57	381.59
648.08	653.14	573.56	205.33	382.57
480.77	522.26	580.68	203.28	382.8
77.52	578.94	583.97	203.83	385.53
383.56	193.06	592.28	204.19	386.75
524.74	489.66	586.8	206.27	387.06
93.88	566.38	594.63	203.06	387.69
538.04	768.96	569.38	207.77	387.71
612.52	585.52	612.49	214.23	387.72
737.95	796.49	575.99	204.54	387.83
406.99	631.81	530.63	205.98	390.17
275.52	127.95	594.13	203.12	390.57
336.86	577.45	936.22	185.12	391.0
437.86	618.21	596.96	207.25	393.73
180.2	301.49	602.89	205.48	394.6
543.16	558.44	579.31	208.25	395.32
347.94	629.12	590.5	209.38	397.97
419.76	555.02	620.61	208.42	404.43
451.33	610.89	609.05	209.87	406.7
502.73	678.23	613.9	211.72	406.89
541.73	671.71	627.73	208.47	407.43
458.33	497.48	635.54	208.41	407.49
604.84	816.32	623.4	211.81	408.04
355.15	496.73	630.31	208.1	409.15

546.63	627.42	625.32	220.23	410.25
904.56	831.71	606.47	212.32	411.07
384.95	568.0	618.35	212.19	415.08
546.75	480.12	663.18	218.11	415.95
288.49	449.49	651.31	211.95	421.23
615.63	492.16	643.03	216.91	424.56
768.64	903.43	655.77	216.3	431.48
708.15	916.75	665.06	215.0	432.64
536.13	528.85	665.82	213.01	432.94
165.04	281.54	670.99	215.4	433.63
980.59	781.59	695.0	212.84	434.36
822.01	850.0	668.58	219.34	438.31
598.71	503.84	1121.25	214.79	442.9
765.95	207.25	955.3	204.91	446.18
634.21	344.71	679.77	219.26	448.74
489.71	731.76	687.86	224.37	449.73
142.42	787.44	704.68	222.94	451.31
591.97	587.53	714.59	224.47	452.24
505.85	511.4	761.84	226.84	456.72
524.4	862.33	732.23	221.62	459.84
846.89	602.9	736.58	223.04	461.61
624.78	923.79	718.48	225.96	464.39
532.43	567.51	734.47	223.05	464.97
525.01	778.66	737.64	225.93	467.42
713.49	512.49	740.48	240.23	471.32
743.09	663.49	778.89	224.86	476.33
628.68	353.96	801.92	230.5	477.5
943.89	708.44	792.95	227.85	488.4
540.44	786.48	789.5	232.34	493.2
522.18	555.78	836.11	242.01	498.48
510.48	497.7	1095.36	207.45	500.58
511.78	541.04	833.78	231.28	500.76
21.34	734.58	1154.9	200.82	504.93
591.13	472.66	911.05	262.49	505.24
547.59	688.57	831.88	234.16	510.2
882.11	684.24	1099.12	212.43	511.88
665.93	971.6	808.61	239.78	512.61
449.52	476.84	838.02	240.79	512.92
852.43	140.98	804.17	241.47	520.56
560.49	626.79	861.86	241.41	522.96
418.72	633.92	858.95	249.15	523.97
720.88	365.64	1246.26	201.48	526.95
747.57	635.52	873.97	239.47	528.9
503.3	624.24	1217.3	208.39	531.68
472.49	176.62	1247.91	218.38	533.18
724.81	441.0	863.56	243.19	534.12
716.68	495.19	1240.49	205.07	534.91
627.07	605.72	899.19	247.41	536.91
490.62	224.51	1292.06	201.13	537.18
676.43	360.9	880.5	244.31	538.99
277.01	641.94	862.96	244.45	541.86
647.94	591.8	1420.54	209.9	544.56
513.0	570.6	1253.11	204.97	545.43
841.46	94.56	1383.22	199.19	547.53
590.13	544.46	1375.38	248.18	548.99
348.81	575.86	1325.52	207.74	549.21
545.62	506.92	927.37	249.7	553.32
444.61	542.51	921.77	244.96	557.36

292.11	477.7	979.63	248.93	557.67
594.92	436.32	1587.47	202.36	559.68
635.44	441.27	945.93	254.37	560.92
610.6	519.62	978.83	260.6	562.55
826.43	786.85	961.51	247.01	573.27
413.7	766.3	1294.54	216.11	574.4
536.0	650.29	1067.53	268.52	576.46
345.97	684.36	927.72	257.14	578.12
456.04	842.48	1329.55	210.68	578.26
730.02	392.53	1402.76	208.26	578.27
471.34	627.44	979.22	269.01	585.64
508.49	558.88	1309.8	212.52	585.86
580.49	152.51	1004.32	245.55	586.61
547.4	464.4	1007.54	257.55	587.84
564.12	668.64	1016.81	257.28	589.12
197.03	510.62	1625.06	204.47	591.82
416.9	656.56	952.26	272.69	595.33
638.14	586.86	1747.86	216.58	595.82
431.2	766.1	996.45	263.89	599.37
552.0	530.35	729.65	261.1	609.37
592.54	829.91	1474.85	212.89	613.4
197.89	915.41	1571.26	216.31	629.08
628.25	630.99	1049.8	270.85	631.74
363.13	865.92	1075.32	266.76	636.55
582.32	630.47	1065.76	268.57	644.54
665.7	681.94	1864.24	214.04	645.11
554.09	494.16	1185.95	291.41	650.48
439.61	450.61	1158.44	270.88	675.2
959.99	631.1	1846.18	215.87	675.99
786.04	859.15	1179.71	272.14	679.81
470.68	671.12	1654.43	232.51	682.57
588.21	448.54	1162.0	293.59	684.39
350.59	425.17	1839.31	215.92	688.7
474.47	476.96	1918.85	209.37	690.36
501.77	728.39	1195.6	293.04	691.18
326.64	536.78	1187.27	283.62	693.53
431.96	482.24	1249.13	279.63	694.78
577.45	661.03	1182.06	282.43	700.14
557.63	247.83	1071.59	287.53	701.9
446.67	629.74	1203.36	293.4	710.93
333.03	433.29	1306.49	295.88	737.71
622.53	532.06	1463.64	314.01	777.46
570.45	464.97	1401.51	310.02	784.06
568.78	640.0	1864.57	281.17	790.19
567.91	689.21	1445.61	305.49	799.47

Appendix D: Additional HR Diagrams

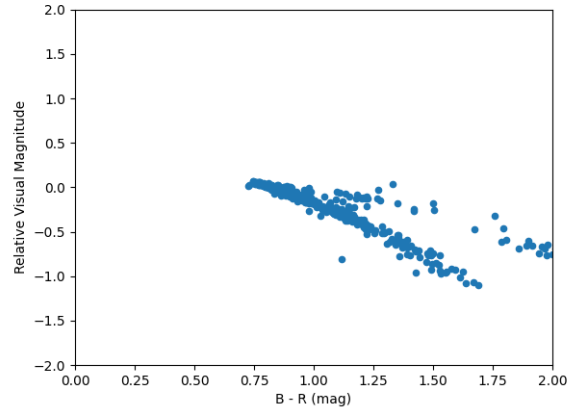


Figure 9: Visual magnitude vs. Color for stars in the Wild Duck cluster. This is a subset of a larger graph; points outside of the ranges seen on the x and y axes were deemed outliers. The zero on the y-axis is defined as the median of all of the magnitudes (including the outliers discarded).

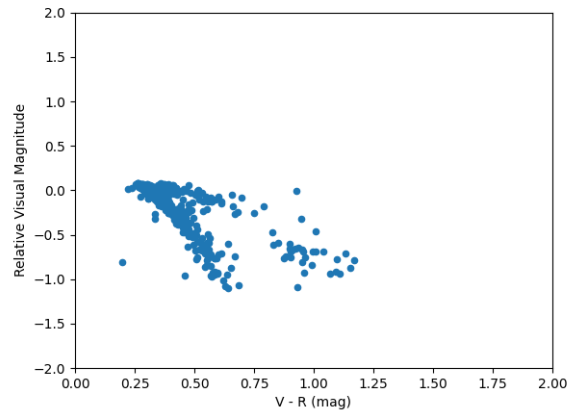


Figure 10: Visual magnitude vs. Color for stars in the Wild Duck cluster. This is a subset of a larger graph; points outside of the ranges seen on the x and y axes were deemed outliers. The zero on the y-axis is defined as the median of all of the magnitudes (including the outliers discarded).

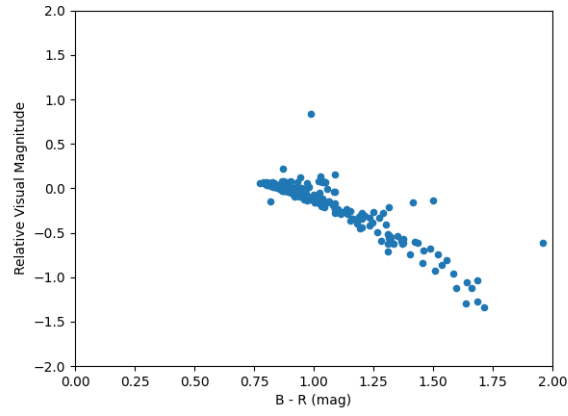


Figure 11: Visual magnitude vs. Color for stars in the M52 cluster. This is a subset of a larger graph; points outside of the ranges seen on the x and y axes were deemed outliers. The zero on the y-axis is defined as the median of all of the magnitudes (including the outliers discarded).

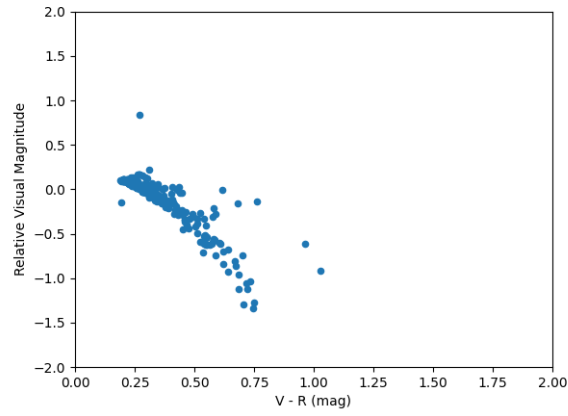


Figure 12: Visual magnitude vs. Color for stars in the M52 cluster. This is a subset of a larger graph; points outside of the ranges seen on the x and y axes were deemed outliers. The zero on the y-axis is defined as the median of all of the magnitudes (including the outliers discarded).

Appendix E: Depiction of the Wild Duck

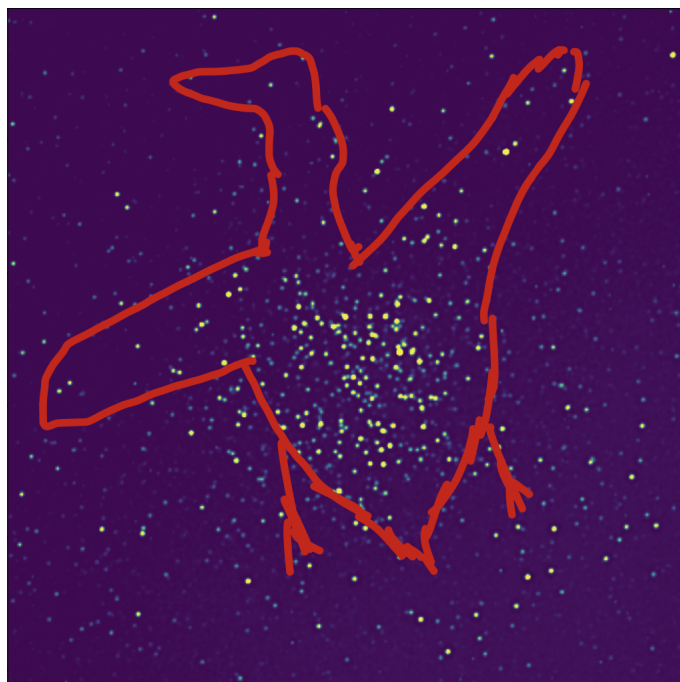


Figure 13: Ze Duck. Artist: Josiah Castillo.